An Effective Automated Grading System for HCC in Biopsy Images

Y. H. Lai[1], P. W. Huang[1*], P. L. Lin[2]
[1]Department of Computer Science,
National Chung Hsing University,
Taichung 40227, Taiwan

[2]Department of Computer Science & Information Management,
Providence University,
Sha-Lu, Taichung 43301, Taiwan

Abstract: Accurate grading for hepatocellular carcinoma (HCC) in biopsy images is important to prognosis and treatment planning. However, visual grading is always time-consuming, subjective, and inconsistent. In this paper, we proposed a novel approach to automatically classifying biopsy images into five grades. At first, a dual morphological reconstruction method was applied to remove noise and accentuate nuclear shapes. Then we used watershed and snake techniques to smoothly segment nuclei from their background. Fourteen features were extracted according to six types of characteristics. We constructed a hierarchical classifier using Support Vector Machine and Sequential Floating Forward Selection method to automatically select an optimal set of features at each decision node of the classifier. Our experimental results demonstrated that 94.5% of accuracy can be achieved for a set of 604 biopsy images.

Key-Words: Hepatocellular Carcinoma, Morphological Reconstruction, Watershed, Snake, Support Vector Machine, Sequential Floating Forward Selection, Hierarchical Classification

1 Introduction

Liver cancer is one of major health problems in the world and still the most deathful disease especially in Taiwan. Hepatocellular Carcinoma (or HCC) is the most common histological type of primary liver cancer. The prognosis and medical treatments are various for different grading of HCC so that accurate pathological discrimination among different grades of HCC becomes very important. However, pathological analysis of tissue is time-consuming and requires correct visual interpretation for microscopic images. Therefore, computer-based analysis for microscopic images is highly desired to provide quantitative, more objective and consistent results for assisting pathologists to improve prognosis and treatment planning.

Many methods for analyzing pathological images have been proposed during the last few years. Beil et al. [1] proposed a dual approach to structural texture analysis for microscopic cell images, in which textures are composed of primitives and can be described by arrangement of regions and lines. Thiran and Macq [2] presented an automatic recognition method based on shape and size analysis for the observed cells in cancerous tissues and provided an evaluation method for scoring the images to be classified. A Biopsy Analysis Support System (BASS) was introduced by Schnorrenberg et al. [3] to detect the nuclei of breast cancer based on staining intensity and the number of stained nuclei. Esgiar et al. [4] developed an algorithm to identify cancerous colon mucosa using six texture features. Weyn et al. [5] developed a computer assisted differential diagnosis system based on syntactic structure analysis, which utilized k-nearest-neighbor (KNN) algorithm with parameters selected from the Voronoi Diagram (VD), Gabriel's Graph (GG), and the Minimum Spanning Tree (MST). A computerized method for grading prostate biopsy images was also reported in [6], which employed multi-wavelet transform and co-occurrence matrices for feature extraction to analyze the entire image instead of individual cells.

In this paper, we present an effective approach to analyzing and grading HCC biopsy images. At first, a dual morphological reconstruction method is applied to the original image to remove noise and accentuate nuclear shapes. Nuclei are smoothly segmented using watershed and snake techniques. Then fourteen features are extracted according to six types of characteristics including nuclear size, nucleocytoplasmic ratio, nuclear irregularity, hyperchromatism, anisonucleosis, and nuclear

* The corresponding author

texture. An optimal feature subset is automatically selected using Support Vector Machine and Sequential Floating Forward Selection method for each decision node of the hierarchical classifier so that biopsy images can be classified effectively. Experimental results showed that 94.5% of accuracy can be achieved for a set of 604 biopsy images with another 200 images as the training set.

2 Image Acquisitions and Segmentation

In this study, every image was obtained by the same processing and acquisition method. Tissue was embedded in paraffin cubes after chemical processing and then cut into very thin sections. These sections were placed on glass slides and stained with colored dyes such as Hematoxylin and Eosin. The images were acquired by a set of equipments including a high-quality optical microscope, a high resolution CCD camera, and an image acquisition computer system. Each image was taken through a microscope with magnifying factor of 400. There were 804 biopsy images with resolution 4080 by 3072 captured by the above procedure. These images were analyzed by an experienced pathologist and classified into five grades (0 to 4) in advance for later comparison.

According to the six types of characteristics for identifying HCC tumor, the major features used for grading are mainly related to cell nuclei; therefore, it is essential to segment nuclei from the images correctly. A HCC biopsy image may contain many undesirable elements such as erythrocyte, leukocyte, and impurities as shown in Fig. 1. In our system, we used a dual morphological reconstruction method to eliminate irrelevances without changing the shapes of nuclei in biopsy images.

Morphological reconstruction [7][8] starts with eroding the original image, and then applies a series of conditional dilations to the marker image using the original image as the conditional image. Morphological reconstruction is more effective than the conventional opening and closing algorithms for removing small blemishes without affecting the shapes of interested objects. The process of morphological reconstruction for a HCC image is shown in Fig. 2, where Fig. 2(a) is the original RGB color image, Fig. 2(b) is the grayscale image in the red plane, Fig. 2(c) is obtained by eroding Fig. 2(b) with a disk shape structure element, Fig. 2(d) is the result from morphological reconstruction using 2(b) and 2(c) as mask and marker images, respectively. Then a second morphological reconstruction procedure (a dilation followed by a series of erosions) is applied by using Fig. 2(d) as the mask image and Fig. 2(e) as the marker image. The final result is shown in Fig. 2(f), where the shapes of nuclei are well preserved and other irrelative objects are removed.

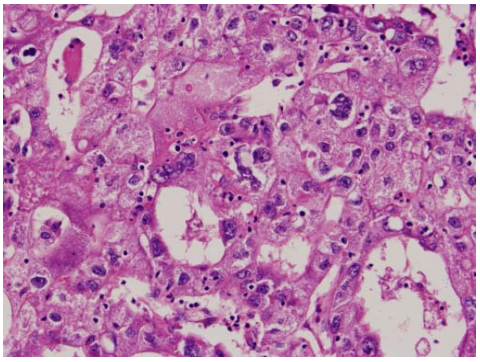

Fig. 1. A HCC biopsy image.

Thresholding methods [9] are usually used for image segmentation. Since the intensities within nuclei and in the background are not uniform as shown in Fig. 3(a), we utilized watershed transform [10] to obtain the edges of nuclei and the snake method [11][12] to smooth those edges. The intuitive idea of watershed transform is to regard a grayscale image as a topographic relief, which is flooded with water starting at the surface global minima. The water level would increase to fill up lower elevation points first. When water coming from different basins would meet, dams called watershed ridge lines are built. An example of watershed transform for nuclei is presented in Fig. 3. Figure 3(b) is the gradient image by performing Sobel operator on Fig. 3(a). The result obtained from watershed segmentation is shown in Fig. 3(c). To refine the contours of nuclei, a snake method [11][12][13] was applied and the final result of segmentation for a biopsy image is shown in Fig. 4.

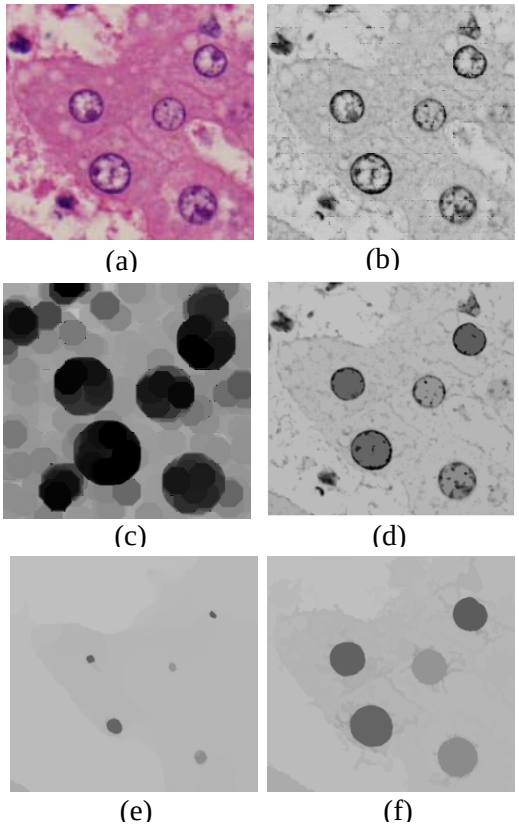

Fig. 2. An example of dual morphological reconstruction.

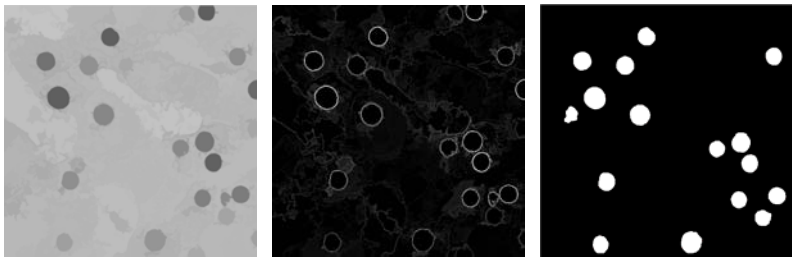

(a) (b) (c)

Fig. 3. An example of watershed transform. (a) Result from morphological reconstruction. (b) The gradient image. (c) Result from watershed segmentation.

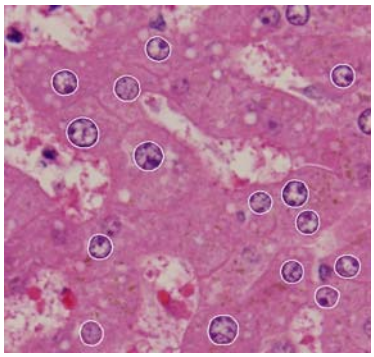

Fig. 4. Final segmentation result from a biopsy image.

3 Features Extraction

The HCC tumor can be classified to five grades (0 to 4) according to six types of nuclear characteristics: nuclear size, nucleocytoplasmic ratio, nuclear irregularity, hyperchromatism, anisonucleosis, and nuclear texture. Grade "0" stands for normal and this number will increase with increasing malignancy level [14][15]. The 14 features derived from these six types of characteristics for automated grading are described below.

Type-1 (Nucleocytoplasmic Ratio):

Nuclear density, nucleus-to-cytoplasm ratio, and cell-size are the three features to be derived from type-1 characteristics. Biopsy images with high HCC grades usually have high nuclear density, high nucleus-to-cytoplasm ratio, and small cell-size. A segmented biopsy image can be envisioned as a complete connected weighted graph, in which nodes are the nuclei and the weight associated with an edge is the distance between two nuclei. Then a Minimum Spanning Tree (MST) [16] T can be found and used as the model for extracting the following three features:

- *Nuclear density (F1):*

$$\left(\sum_{(u,v)\in T} w(u,v)\right) \Big/ \left(|V|-1\right) \tag{1}$$

- *Nucleus-to-Cytoplasm ratio (F2):*

$$\sum_{v\in T}\left(area\_n(v) \Big/ area\_c(v)\right) \Big/ |V| \tag{2}$$

- *Cell size (F3):*

$$\sum_{v\in T}\left(area\_n(v)+area\_c(v)\right) \Big/ |V| \tag{3}$$

In the above equations, (u,v) is an edge in T, $w(u,v)$ is the distance between nucleus u and v, $area\_n(v)$ and $area\_c(v)$ stand for the area of nucleus v and its cytoplasm, respectively; and $|V|$ is the number of nuclei. In our MST model, a cytoplasm area can be estimated by extending the boundaries of two neighboring nuclei until they meet at the middle point of their virtual connecting edge.

Type-2 (Nuclear Irregularity):

Shape is one of the most important low-level image features to human perception. Because of serious deformity, the shapes of nuclei are no longer kept round in cancerous tissues. Therefore, we extract three numerical values for estimating irregularity of a nucleus as follows:

- *Circularity (F4)* [17]:

$$4\times\pi\times\frac{Area}{Circumference^2} \tag{4}$$

- *Area irregularity (F5):* There are four intersecting points between a nucleus and its Minimum Bounding Rectangle (MBR) as shown in Fig. 5. If the intersecting point is on a vertical (horizontal) side of the MBR, a horizontal (vertical) cutting line will go through this point. Consequently, four possibly overlapping areas will be formed with each area surrounded by a segment of nucleus's boundary, a vertical line, and a horizontal line. Irregularity of nucleus can be reflected by

$$\frac{1}{4}\sum_{i=1}^{4}\min_{j=1\ldots4,\, j\neq i}\left|area(Si)-area(Sj)\right| \tag{5}$$

- *Contour irregularity (F6):* Since a nuclear shape is quite smooth, it can be represented by a sequence of sampling boundary points $\{p_0\ p_1\ p_2 \ldots p_{j-w}\ \ldots\ p_j\ \ldots p_{n-1}\}$ with $p_t=p_{t+n}$ for $t=\ldots\ -1\ 0\ 1\ldots$. Curvature at a boundary point $p_j=(x_j\ y_j)$ can be approximated by the differentiation of two successive tangent values in window w [18]:

$$d_j = \tan^{-1}\frac{y_j - y_{j-w}}{x_j - x_{j-w}} - \tan^{-1}\frac{y_{j-1} - y_{j-1-w}}{x_{j-1} - x_{j-1-w}}$$

Then we define contour irregularity as

$$\sum_{j=0}^{n-1}\left|d_j - d_{j-1}\right| \quad (6)$$

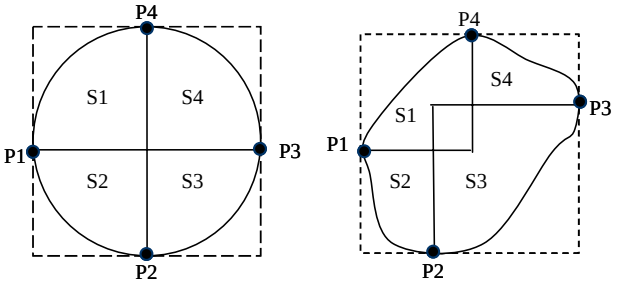

(a) (b)

Fig. 5. Two examples of area irregularity. (a) A round nucleus. (b) An irregular nucleus.

Type-3 (Hyperchromatism):

Hyperchromatism represents excessive pigmentation in hemoglobin content of erythrocytes. It is an important characteristic appearing in a malignant tumor. For the case of higher grade HCC, chromatin abnormality will increase the staining capacity by staining colored dyes especially in cell nuclei. By taking the advantage of reflecting the amount of chromatin within nuclei, we can obtain the following two features:

- *Average intensity (F7):* the intensity of nuclei in higher grade HCC appears darker than that of normal nuclei. Thus, the average intensity reflects the degree of dyeing for nuclear staining and can be easily extracted from gray-level nuclei.
- *B/D spot ratio (F8):* Within a malignant tumor, increasing chromatin will cause more holes to occur. The holes are reflected by the ratio of bright and dark spots in nucleus. The bright and dark spots can be found by using top-hat and bottom-hat transforms [19], respectively.

Type-4 (Nuclear Size):

- *Area (F9):* HCC with higher grade implies a higher probability of larger nuclei. Therefore, nuclear size is also used as a criterion for HCC grading and can be obtained by simply counting the number of pixels in nucleus.

Type-5 (Anisonucleosis):

In cases of HCC with high grades, the variance among the areas of nuclei is noticeable. Thus, the following two features can be derived from size distribution of nuclei for identifying HCC with high grades.

- *Standard deviation of nuclear size (F10):* This feature is calculated by the squared root of the average squared deviation from the mean nuclear size.
- *Difference of extreme nuclear sizes (F11):* Sometimes in grade-4 HCC images, there are only a few nuclei having large area differences. So the standard deviation of nuclear size can not represent anisonucleosis effectively. In this case, we use the difference between the maximal and minimal areas of nuclei as anisonucleosis.

Type-6 (Nuclear Texture):

Gray Level Co-occurrence matrices (GLCM) have been shown to be useful in texture analysis [20][21][22]. For nuclear texture analysis, the following three features are derived from a GLCM N_d with neighboring pixels separated by a distance d in direction θ. In our implementation, we chose $d=1$ and $\theta=0^o, 45^o, 90^o, 135^o$.

- *Uniformity Energy (F12):*

$$\sum_i\sum_j N_d^2[i,j] \quad (7)$$

- *Contrast (F13):*

$$\sum_i\sum_j (i-j)^2 N_d[i,j] \quad (8)$$

- *Homogeneity (F14):*

$$\sum_i\sum_j \frac{N_d[i,j]}{1+|i-j|} \quad (9)$$

4 Classification

This study investigated the performance of two classifiers. One is to directly use SVM once to classify biopsy images into five grades by using all fourteen features. The other is to construct a hierarchical classifier so that each decision node has an optimal feature subset automatically selected by Support Vector Machine [23][24] and Sequential Floating Forward Selection method [25].

Support Vector Machine is a popular classification and regression technique [23]. The basic idea of SVM is to transform data into a higher dimensional space and find the optimal hyperplane with maximal separation margin between classes. In this study, the implementation of SVM used for experiments is LIBSVM [24].

Conventional image classification methods use a fixed number of features for classifying images. However, for HCC grading, the features used for identifying various grades are different. For example, texture is the best among the 14 features if we want to distinguish grade 0 from grade 1 while nucleocytoplasmic ratio is the best if we want to distinguish grade 1 from grade 3. Therefore, we propose a hierarchical structure shown in Fig. 6 as the classifier for distinguishing all five grades. Our approach can prevent irrelative or insignificant features from being selected to reduce the dimension of feature space while avoiding possible interferences during the decision process. Sequential Floating Forward Selection (SFFS) method is used to help choosing a subset of features so that the feature space is optimally reduced according to a certain evaluation criterion [25][26]. The basic idea of SFFS is based on the *"plus l - take away r"* concept [27], which can be implemented by a procedure with each Sequential Forward Selection step followed by a number of Sequential Backward Selection steps as long as the resulting subset is better than the previously evaluated ones at that level. The optimal feature subset associated with each node of the classifier is shown in Table 1. At each node, an optimal subset of features was selected from the 14 features so that the two extreme grades can be effectively distinguished by those selected features. For instance, the two extreme grades are G_0 and G_4 at the root node, which can be distinguished by the set of optimal features FS_1={F3-F5, F7, F9, F12}. The two extreme grades for the right child of the root node are G_1 and G_4, which can be differentiated by the set of optimal features FS_3={F3-F5, F7, F8, F10, F11, F13}. Thus we can easily obtain the classification result for any biopsy image through a sequence of four decision-making steps.

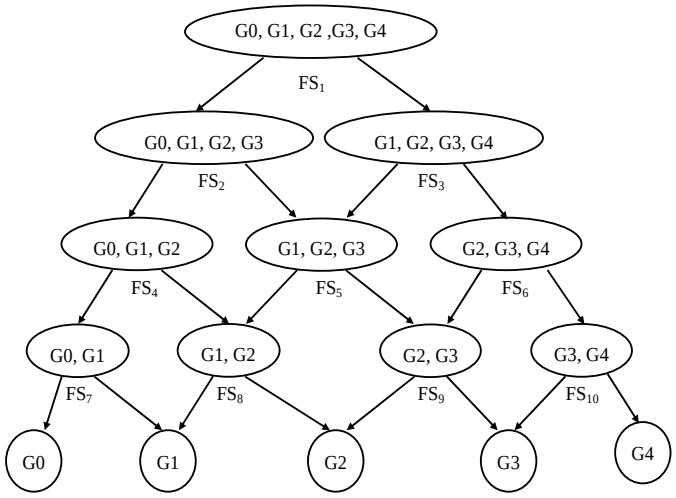

Fig. 6. The hierarchical classifier for HCC grading.

5 Experimental Results

We have evaluated the performance of our HCC grading system using 604 biopsy images. There are five possible grades from G_0 to G_4. To establish the ground truth, the images were graded by an expert pathologist in advance. For convenience of easy process, each image was divided into 12 equal parts, and the fourteen features were extracted from each part individually. Sometimes, there is more than one grade appearing in different parts of the same image. If such a case occurred, the highest grade was considered and recorded.

Table 2 shows the result of our classification method. There are 604 biopsy images in total; among them 58 images were graded as G_0, 26 images were graded as G_1, 75 images were graded as G_2, 220 images were graded as G_3, and 225 images were graded as G_4 by an experienced pathologist. We used 200 images as the training set and another 604 images for testing. Our classifier has 100 % accuracy

Table 1. Optimal feature subsets at each criteria node.

	F1	F2	F3	F4	F5	F6	F7	F8	F9	F10	F11	F12	F13	F14
FS_1			✓	✓	✓		✓		✓			✓		
FS_2	✓	✓	✓	✓	✓		✓		✓				✓	✓
FS_3			✓	✓	✓		✓	✓		✓	✓		✓	
FS_4	✓	✓		✓	✓	✓	✓		✓		✓			
FS_5	✓	✓	✓	✓	✓					✓		✓	✓	
FS_6		✓	✓	✓	✓		✓		✓	✓	✓	✓	✓	✓
FS_7		✓	✓	✓		✓	✓	✓	✓			✓		✓
FS_8					✓		✓	✓	✓	✓		✓	✓	✓
FS_9	✓	✓	✓	✓			✓	✓	✓			✓	✓	✓
FS_{10}	✓	✓	✓	✓	✓	✓	✓	✓	✓	✓	✓	✓	✓	✓

Table 2. Performance results of our hierarchical classifier.

Grades	Visual Grading	Classification results using our method					
		G_0	G_1	G_2	G_3	G_4	Accuracy
G_0	58	58	0	0	0	0	100. %
G_1	26	0	26	0	0	0	100. %
G_2	75	0	0	72	2	1	96.0 %
G_3	220	0	1	0	201	18	91.4 %
G_4	225	0	0	6	5	214	95.0 %
Total	604	58	27	78	208	233	94.5 %

in grading G_0 and G_1. The lowest accuracy is 91.4% in grading G_3. It seems that our method is more "aggressive" as compared to manual grading because 18 out of 220 images were classified as G_4 instead of G_3. On an average, the overall accuracy is 94.5% for classifying 604 biopsy images. In addition, the performance of our classifier is better than of a SVM. Figure 7 shows the comparison result between a SVM classifier and our hierarchical classifier for HCC grading with a training set of size 50, 75, 100, 125, 150 images, respectively. The result shows that our hierarchical classifier with optimal subset of features in each decision node always has higher accuracy than SVM using a fixed number of 14 features.

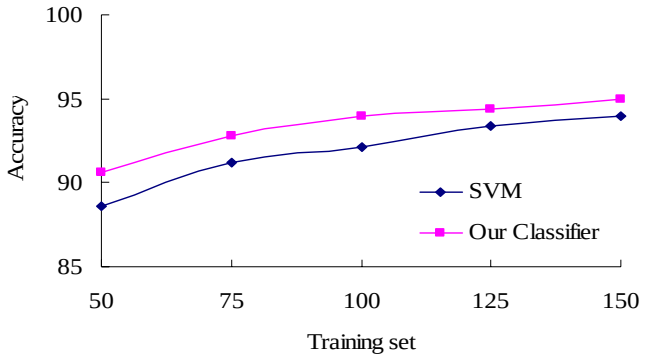

Fig. 7. Comparison between SVM and our hierarchical classifier.

6 Conclusions

Accurate grading for hepatocellular carcinoma (HCC) in biopsy images is important to prognosis and treatment planning. Visual grading by human beinsgs is time-consuming, subjective, and inconsistent while computerized HCC analysis for biopsy images is a very complex task requiring a lot of appropriate image processing steps and experts' domain knowledge for correct justification. In this paper, we proposed a novel approach to automatically classifying HCC in biopsy images into five grades. In image preprocessing, a dual morphological reconstruction method was applied to remove noise and accentuate nuclear shapes. Nuclei were segmented from images using watershed and snake techniques. Such a hybrid approach is robust in terms of removing noise and preserving shapes of nuclei in an effective way. Fourteen features were then extracted from segmented biopsy images according to six types of characteristics. A hierarchical classifier was built to automatically classify HCC in biopsy images into five grades so that benignancy and various degrees of malignance can be distinguished. To make sure the classifier should have an effective performance, Sequential Floating Forward Selection method was adopted to select an optimal feature subset for the Support Vector Machine associated with every decision node at each stage of classification. Our experimental results demonstrated that 94.5% of accuracy can be achieved for a set of 604 biopsy images. The results also showed that our method has higher accuracy than the simple SVM classifier directly using the fourteen features.

References:

[1] Michael Beil, Theano Irinopoulou, Jany Vassy, and Gunter Wolf, A Dual Approach to Structural Texture Analysis in Microscopic Cell Images, *Computer Methods and Programs in Biomedicine*, Vol. 48, No. 3, Dec. 1995, pp. 211-219.

[2] Jean-Philippe Thiran and Benoit Macq, Morphological Feature Extraction for the Classification of Digital Images of Cancerous Tissues, *IEEE Transactions on Biomedical Engineering*, Vol. 43, No. 10, Oct. 1996, pp. 1011-1020.

[3] Frank Schnorrenberg, Constantinos S. Pattichis, Kyriacos C. Kyriacou, and Christos N. Schizas, Computer-Aided Detection of Breast Cancer Nuclei, *IEEE Transactions on Information Technology in Biomedicine*, Vol. 1, No. 2, Jun. 1997, pp. 128-140.

[4] Abdelrahim Nasser Esgiar et al., Microscopic Image Analysis for Quantitative Measurement

and Feature Identification of Normal and Cancerous Colonic Mucosa, *IEEE Transactions on Information Technology in Biomedicine*, Vol. 2, No. 3, Sep. 1998, pp. 197-203.

[5] Barbara Weyn et al., Computer-Assisted Differential Diagnosis of Malignant Mesothelioma Based on Syntactic Structure Analysis, *Cytometry*, Vol. 35, No. 1, Jan. 1999, pp. 23-29.

[6] Kourosh Jafari-Khouzani and Hamid Soltanian-Zadeh, Multiwavelet Grading of Pathological Images of Prostate, *IEEE Transactions on Biomedical Engineering*, Vol. 50, No. 6, Jun. 2003, pp. 697-704.

[7] R. M. Haralick, S. R. Sternberg, and X. Zhuang, Image Analysis Using Mathematical Morphology, *IEEE Transactions on Pattern Analysis and Machine Intelligence*, Vol. 9, No. 4, Jul. 1987, pp. 532-550.

[8] Vincent Luc, Morphological Grayscale Reconstruction in Image Analysis: Applications and Efficient Algorithms, *IEEE Transactions on Image Processing*, Vol. 2, No. 2, Apr. 1993, pp. 176-201.

[9] Mehmet Sezgin and Bulent Sankur, Survey Over Image Thresholding Techniques and Quantitative Performance Evaluation, *Journal of Electronic Imaging*, Vol. 13, No. 1, Jan. 2004, pp. 146-165.

[10] Jos B.T.M. Roerdink and Arnold Meijster, The Watershed Transform: Definitions, Algorithms and Parallelization Strategies, *Fundamenta Informaticae*, Vol. 41, No. 1-2, Jan. 2000, pp. 187-228.

[11] Michael Kass, Andrew Witkin, and Demetri Terzopoulos, Snake: Active Contour Models, *International Journal of Computer Vision*, Vol. 1, No. 4, 1987, pp. 321-331.

[12] Chenyang Xu and Jerry L. Prince, Snakes, Shapes, and Gradient Vector Flow, *IEEE Transactions on Image Processing*, Vol. 7, No.3, Mar. 1998, pp. 359-369.

[13] Dzung L. Pham, Chenyang Xu, and Jerry Prince, A Survey of Current Methods in Medical Image Segmentation, *Annual Review of Biomedical Engineering*, Vol. 2, Jan. 2000, pp. 315-337.

[14] Ugochukwu C. Nzeako et al., Tumor Pathology and Survival in HCC, *Cancer*, Vol. 74, No. 4, Mar. 1995, pp. 579-588.

[15] Kamal G. Ishak, Zachary D. Goodman, and J. Thomas Stocker, *Tumors of the Liver and Intrahepatic Bile Ducts*. Washington DC: Armed Forces Institute of Pathology, 2001.

[16] Thomas H. Cormen, Charles E. Leiserson, Ronald L. Rivest, and Clifford Stein, *Introduction to Algorithms, Second Edition*, MIT Press and McGraw-Hill, 2001.

[17] Murk J. Bottema, Circularity of Objects in Images, *The 2000 IEEE International Conference on Acoustics, Speech, and Signal Processing*, Vol. 6, Jun. 2000, pp. 2247-2250.

[18] Hannu Kauppinen, Tapio Seppanen, and Matti Pietikainen, An Experimental Comparison of Autoregressive and Fourier-Based Descriptors in 2D Shape Classification, *IEEE Transactions on Pattern Analysis and Machine Intelligence*, Vol. 17, No. 2, Feb. 1995, pp. 201-207.

[19] A. Moragas, M. Garcia-Bonafe, I. de Torres, and M. Sans, Textural Analysis of Lymphoid cells in serous effusions. A Mathematical Morphologic Approach, *Analytical and Quantitative Cytology and Histology*, Vol. 15, No. 3, Jun. 1993, pp. 165-170.

[20] Robert Haralick, K. Shanmugam, and Its'hak Dinstein, Texture Features for Image Classification, *IEEE Transactions on Systems, Man, and Cybernetics*, Vol. SMC-3, No. 6, Nov. 1973, pp. 610-621.

[21] Robert Haralick, Statistical and Structural Approaches to Texture, *Proceedings of the IEEE*, Vol. 67, No. 5, May 1979, pp. 786-804.

[22] Linda G. Shapiro and George C. Stockman, *Computer Vision*, Prentice Hall, 2001.

[23] Christopher J.C. Burges, A Tutorial on Support Vector Machines for Pattern Recognition, *Data Mining and Knowledge Discovery*, Vol. 2, No.2, Jun. 1998, pp. 121-167.

[24] Chih-Chung Chang and Chih-Jen Lin, LIBSVM: A Library for Support Vector Machines, 2001. Software available at http://www.csie.ntu.edu.tw/~cjlin/libsvm.

[25] P. Pudil, F. Ferri, J. Novovicova, and J. Kittler, Floating Search Methods for Feature Selection with Nonmonotonic Criterion Functions, *Proceedings of the 12th IAPR International, Conference on Pattern Recognition, Vol. 2 - Conference B: Computer Vision & Image Processing*, Oct. 1994, pp. 279-283.

[26] Mineichi Kudo and Jack Sklansky, Comparison of Algorithms that Select Features for Pattern Classifiers, *Pattern Recognition*, Vol. 33, No. 1, Jan. 2000, pp. 25-41.

[27] S. D.Stearns, On Selecting Features for Pattern Classifiers, *3rd International Conference on Pattern Recognition*, 1976, pp. 71-75.